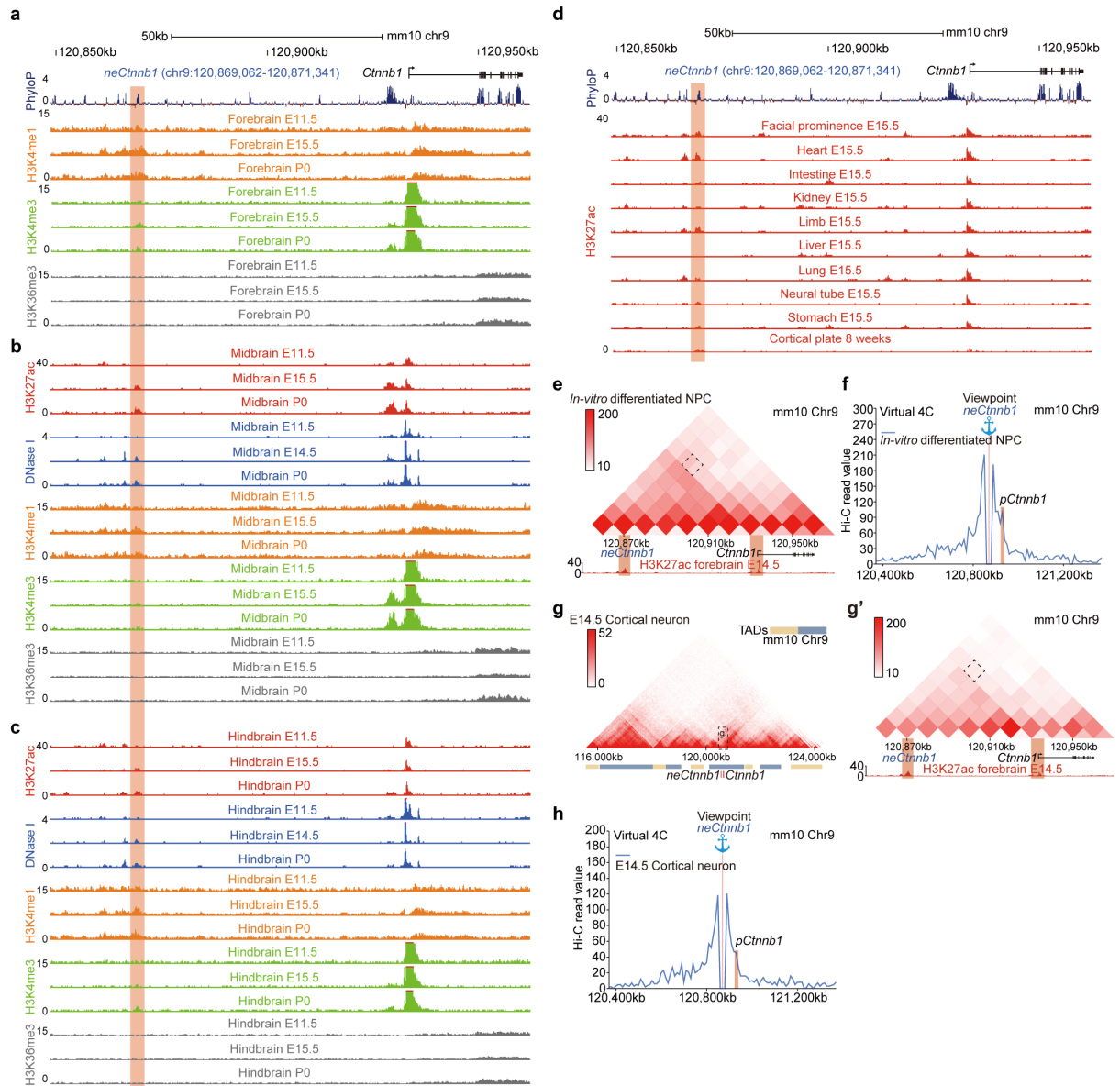


Supplementary information

1
2
3
4
5
6
7
8
9

A *Cttnb1* enhancer regulates neocortical neurogenesis by controlling the abundance of intermediate progenitors

Junbao Wang^{1,#}, Andi Wang^{1,#}, Kuan Tian¹, Xiaojiao Hua¹, Bo Zhang¹, Yue Zheng¹,
Xiangfei Kong¹, Wei Li¹, Lichao Xu¹, Juan Wang², Zhiqiang Li¹, Ying Liu^{1,*}, Yan Zhou^{1,*}

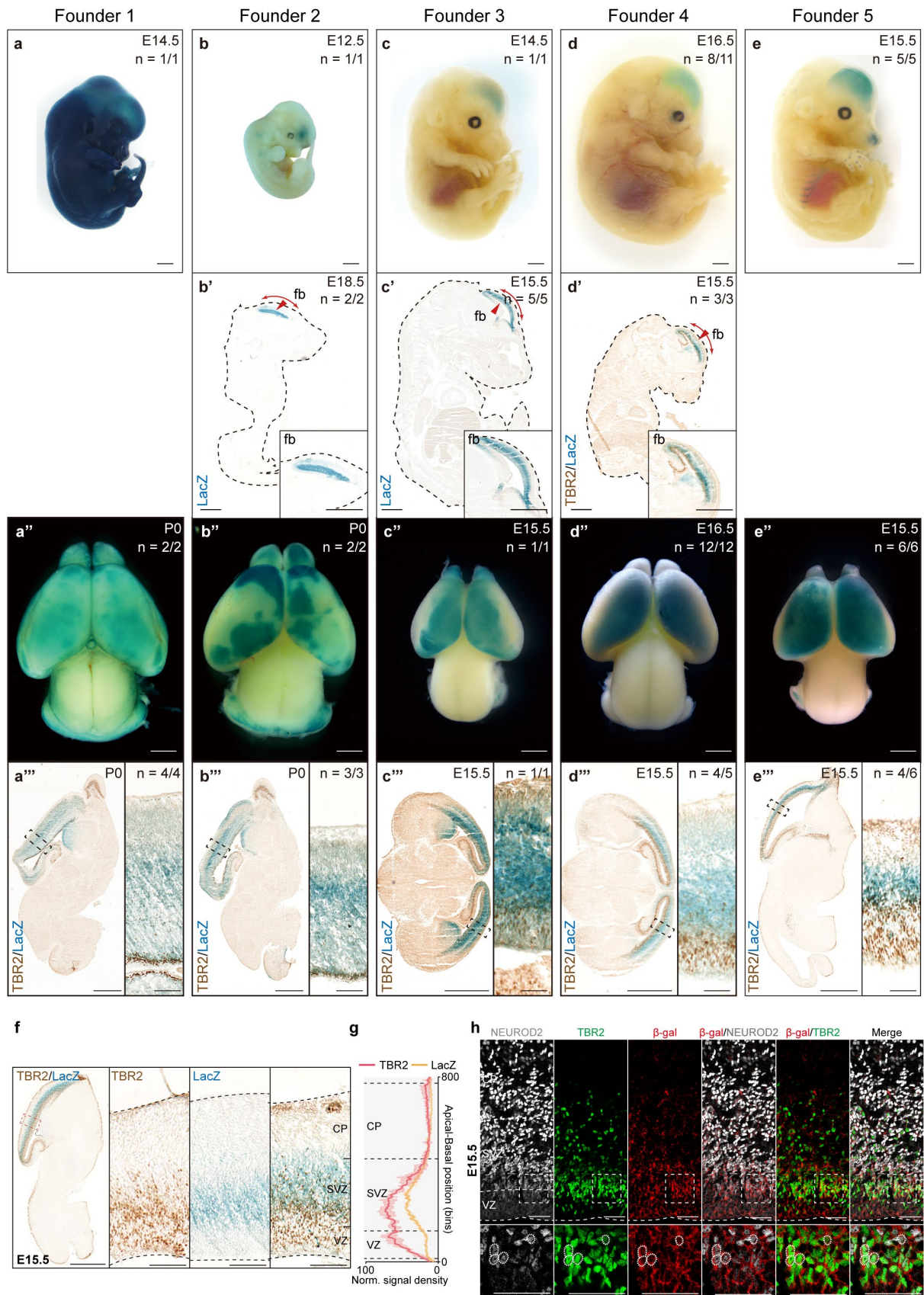


10

11 **Supplementary Figure S1. *neCtnnb1* is a putative enhancer upstream of *Ctnnb1*.**

12 **a-c** Schematic representation of the upstream region of mouse *Ctnnb1* gene and the
 13 location of putative enhancer *neCtnnb1* (orange shading). Enrichment of indicated
 14 signals in developing forebrains (**a**), midbrains (**b**) and hindbrains (**c**) were shown.
 15 Data were obtained from ENCODE. **d** Enrichment of H3K27ac ChIP-seq signals in
 16 indicated tissues of E15.5 embryos. Data were obtained from ENCODE. **e-f** The Hi-C
 17 data (**e**) and virtual 4C (**f**) of *in-vitro* differentiated NPCs revealing the interaction
 18 between *neCtnnb1* and *pCtnnb1*. **g** The Hi-C data of E14.5 cortical neurons were
 19 obtained from the 3D genome browser. Boundaries of TADs and locations of *neCtnnb1*
 20 and *Ctnnb1* gene (red bars) are indicated below. **g'** Regions magnified from (**g**). Boxed
 21 area indicating the interaction between *neCtnnb1* and *pCtnnb1*. **h** Virtual 4C of E14.5
 22 cortical neurons revealing the interaction between *neCtnnb1* and *pCtnnb1*.

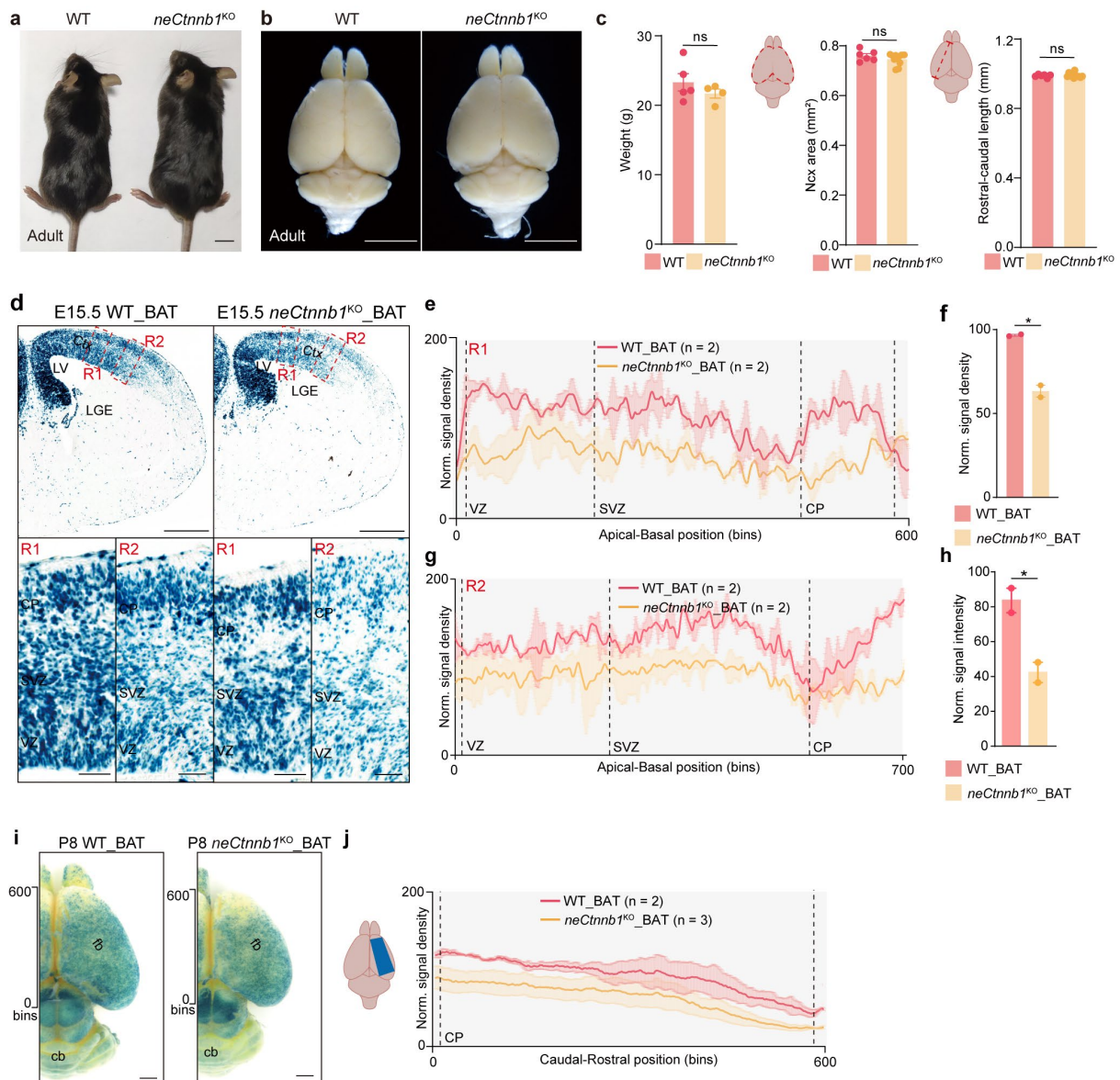
23



24
25
26

Supplementary Figure S2. *neCtnnb1* is predominantly active in developing neocortex.

27 **a-e** X-Gal staining (blue) of whole embryos (**a-e**), sagittal whole-body sections (**b'-d'**),
28 brains (**a''-e''**) and sagittal/coronal brain sections (**a'''-e'''**) of *neCtnnb1-LacZ-iCre*
29 reporter mice. Due to the influence of integration sites and copy numbers on
30 expression, the reporter activity in a specific tissue was only considered reliable when
31 it was found in at least two or more independent individual embryos. **f** E15.5 sagittal
32 brains sections of *neCtnnb1-LacZ-iCre* mice were sequentially stained with LacZ/ β -
33 Gal (blue) for *neCtnnb1* activity and TBR2 (brown), with boxed Ncx regions magnified
34 on right panels. **g** Quantifications of normalized signal density of β -Gal and TBR2
35 signals in (**f**). **h** Immunofluorescence of NEUROD2 (gray), TBR2 (green), and β -Gal
36 (red) on coronal sections of E15.5 *neCtnnb1-LacZ-iCre* Ncx. Scale bars, 1mm (**a-e**,
37 **b'-d'**, **a''-e''**, **a'''-e'''** and **f**), 100 μ m (magnified views in **a'''-e'''** and **f**), 50 μ m (**h**).
38

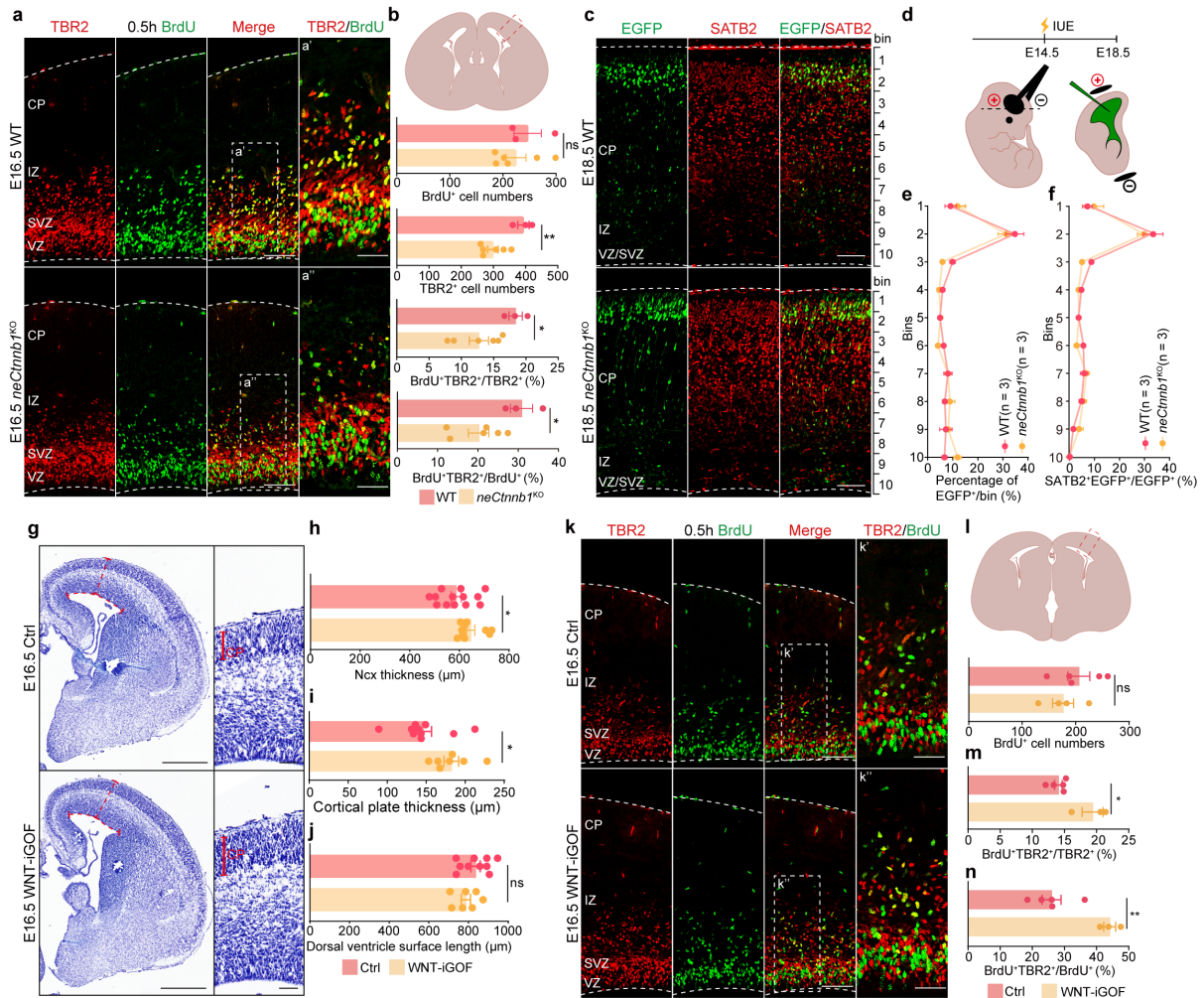


39

40 **Supplementary Figure S3. Knockout of *neCtnnb1* compromised *Ctnnb1*'s**
 41 **reporter activity in developing neocortices.**

42 **a** Representative images of adult (8 weeks) WT and *neCtnnb1*^{KO} mice. **b** Dorsal views
 43 of adult WT and *neCtnnb1*^{KO} mouse brains. **c** Quantifications of adult WT and
 44 *neCtnnb1*^{KO} mice in body weight, neocortex area and length. n = 5 for WT brains and
 45 n = 4 for *neCtnnb1*^{KO} brains. Each point represents an individual brain. **d** X-Gal
 46 staining (blue) on E15.5 coronal sections of WT_BAT (left) and *neCtnnb1*^{KO}_BAT (right)
 47 Ncx, with boxed regions (R1s and R2s) magnified on the bottom. **e-h** Quantification of
 48 normalized signal density of LacZ in two boxed regions of (**d**). n = 2 for WT_BAT brains
 49 and n = 2 for *neCtnnb1*^{KO}_BAT brains. Each point represents an individual brain. **i** X-
 50 Gal staining (blue) in P8 WT_BAT (left) and *neCtnnb1*^{KO}_BAT (right) whole mount
 51 brains. **j** Quantification of normalized signal density of LacZ in boxed regions of (**i**). n

52 = 2 for WT_BAT brains and n = 3 for *neCtnnb1*^{KO}_BAT brains. Each point represents
53 an individual brain. Quantification data are shown as mean ± SEM. Statistical
54 significance was determined using an unpaired two-tailed Student's *t*-test (**c**, **f** and **h**)
55 **P* < 0.05, ***P* < 0.01, and ****P* < 0.001. ns, not significant. Scale bars, 1 cm (**a** and **i**),
56 500 μm (**b** and **d**), 50 μm (magnified views in **d**).
57

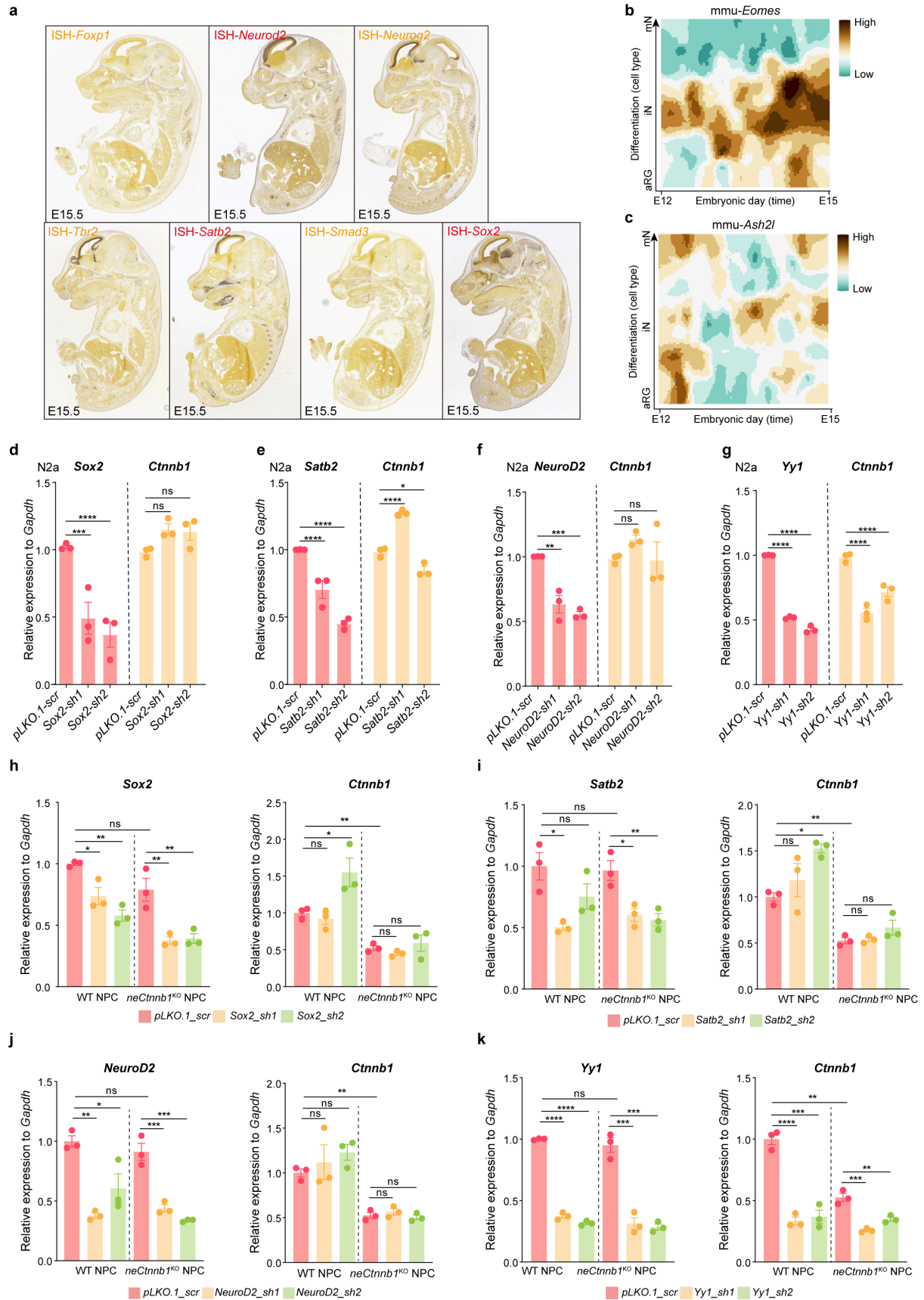


58

59 **Supplementary Figure S4. *neCtnnb1* regulates neocortical neurogenesis and IP**
 60 **divisions.**

61 **a-b** Immunofluorescence (**a**) and quantification (**b**, top) of BrdU⁺ (green) and TBR2⁺
 62 (red) cells on boxed area of coronal sections (**b**) of E16.5 WT and *neCtnnb1*^{KO} Ncx.
 63 Pregnant mice were injected with BrdU 30 min before sacrifice. n = 3 for WT brains
 64 and n = 6 for *neCtnnb1*^{KO} brains. Each point represents an individual brain. **c**
 65 Immunofluorescence of SATB2⁺ (red) and EGFP⁺ (green) cells on E18.5 coronal
 66 sections of WT and *neCtnnb1*^{KO} Ncx. Neocortex were electroporated with EGFP-
 67 expressing constructs at E14.5. **d** Schematic diagram illustrating the strategy of *in*
 68 *utero* electroporation (IUE) of WT and *neCtnnb1*^{KO} embryos. **e-f** Neocortices shown in
 69 (**c**) were divided into 10 bins of equal height and fixed width, and EGFP⁺ (green) cells
 70 in each bin were counted and quantified. n = 3 for WT brains and n = 3 for *neCtnnb1*^{KO}
 71 brains. Each point represents an individual brain. **g** Nissl-staining on E16.5 coronal
 72 sections of Ctrl and WNT-iGOF Ncx. **h** Comparison of neocortical thickness of E16.5
 73 Ctrl and WNT-iGOF mice. n = 13 for Ctrl brains and n = 10 for WNT-iGOF brains. Each
 74 point represents an individual brain. **i** Comparison of cortical plate thickness of E16.5

75 Ctrl and WNT-iGOF mice. n = 10 for Ctrl brains and n = 7 for WNT-iGOF brains. Each
76 point represents an individual brain. **j** Comparison of dorsal ventricle surface length of
77 E16.5 Ctrl and WNT-iGOF mice. n = 10 for Ctrl brains and n = 7 for WNT-iGOF brains.
78 Each point represents an individual brain. **k-n** Immunofluorescence (**k**) and
79 quantification (**l-n**) of TBR2+ (red) and BrdU+ (green) cells on boxed area of coronal
80 sections (**l**) of E16.5 Ctrl and WNT-iGOF Ncx. Pregnant mice were injected with BrdU
81 30 min before sacrifice. Each point represents an individual brain. Quantification data
82 are shown as mean \pm SEM. Statistical significance was determined using unpaired
83 two-tailed Student's *t*-test (**b**, **h**, **i**, **j**, **l**, **m** and **n**); two-way ANOVA followed by Sidak's
84 multiple comparisons test (**e** and **f**). **P* < 0.05, ***P* < 0.01, ****P* < 0.001, and *****P* <
85 0.0001. ns, not significant. Scale bars, 500 μ m (**g**), 100 μ m (**a**, **c**, **k** and magnified
86 views in **g**), 50 μ m (magnified views in **a** and **k**).
87



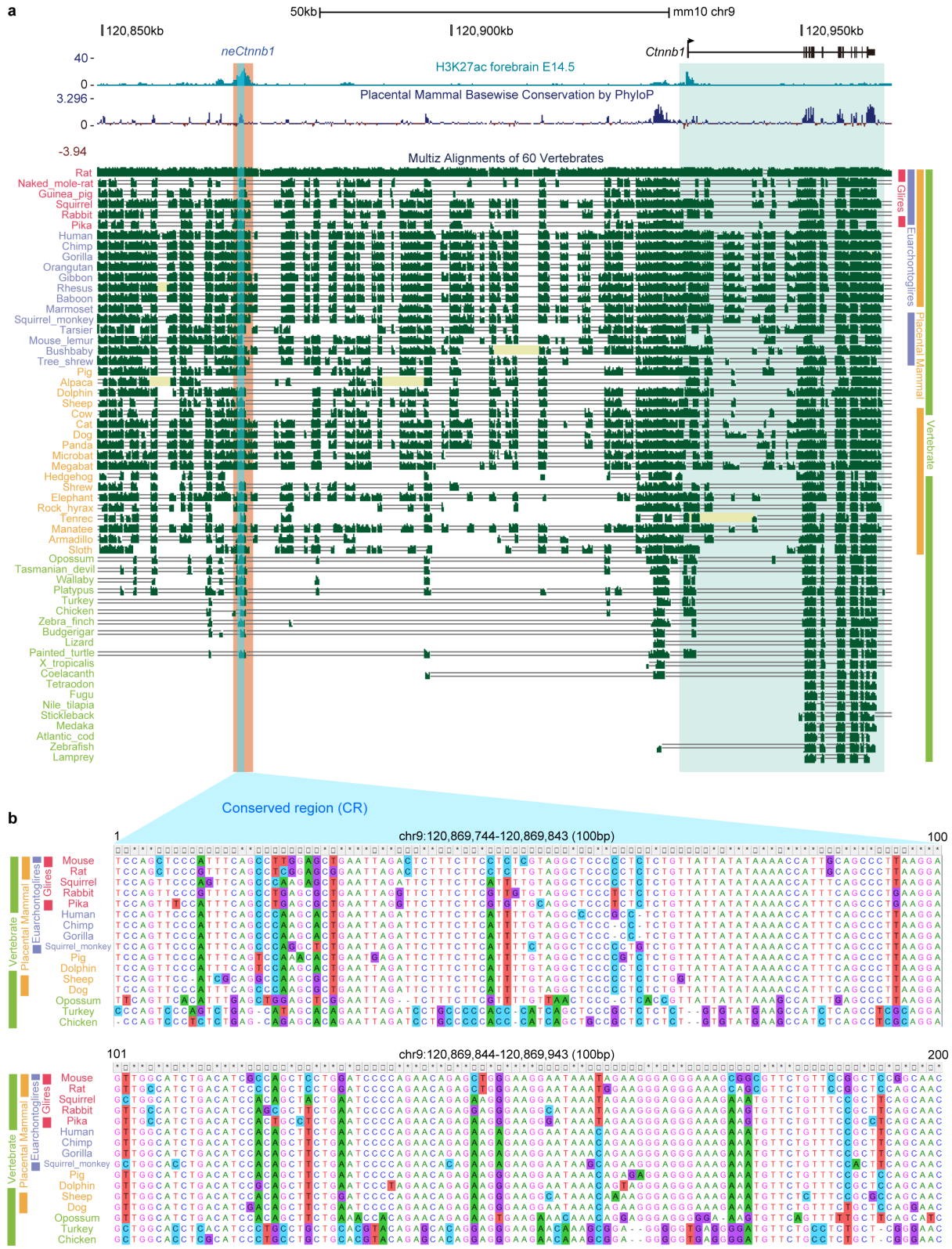
88

89 **Supplementary Figure S5. Effects of selected *trans*-acting factors on**

90 **expressions of *Ctnnb1*.**

91 **a** Representative images showing *in situ* hybridization (ISH) of *Foxp1*, *Neurod2*,
92 *Neurog2*, *Tbr2*, *Satb2*, *Smad3* and *Sox2* on sagittal sections of E15.5 mouse embryos.
93 Data were extracted from the Allan Brain Atlas. **b-c** Expression patterns of *Eomes* (**b**)
94 and *Ash2l* (**c**) during mouse neocortical neurogenesis. Visualized single-cell RNA-seq
95 data were extracted from Humous.org (<http://www.humous.org/>). **d-g** RNA levels of
96 *Sox2* (**d**), *Satb2* (**e**), *NeuroD2* (**f**), *Yy1* (**g**) and *Ctnnb1* in Neuro-2a transfected with
97 indicated vectors for two days. Each point represents an independent experiment. **h-**
98 **k** RNA levels of *Sox2* (**h**), *Satb2* (**i**), *NeuroD2* (**j**), *Yy1* (**k**) and *Ctnnb1* in WT and
99 *neCtnnb1*^{KO} neocortical NPCs transfected with indicated vectors for two days. NPCs
100 were derived from E12.5 Ncx. n = 3 for WT brains and n = 3 for *neCtnnb1*^{KO} brains.
101 Each point represents NPCs derived from an individual brain. Quantification data are
102 shown as mean ± SEM. Statistical significance was determined using two-way ANOVA
103 followed by Sidak's multiple comparisons test. (**d-k**). **P* < 0.05, ***P* < 0.01, ****P* <
104 0.001, and *****P* < 0.0001. ns, not significant.

105

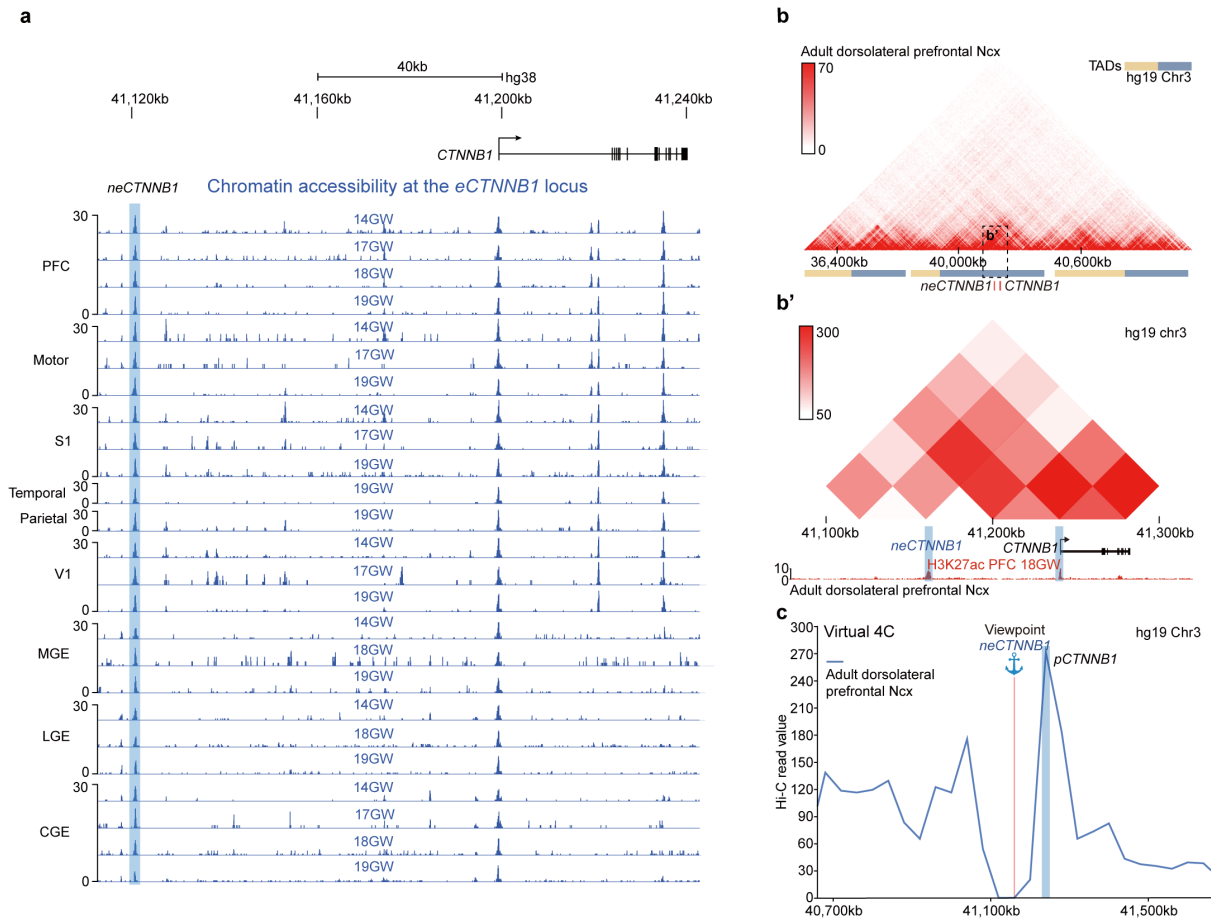


Supplementary Figure S6. Sequence conservation of *neCtnnb1*.

a UCSC genome browser track depicts conservation of *neCtnnb1* among vertebrates.

b Multiple sequence alignment of the core conserved region of *neCtnnb1* among

selected vertebrates. Data were extracted from the UCSC genome browser.



111

112 **Supplementary Figure S7. *neCTNNB1* interacts with *pCTNNB1* in developing**
 113 **human brains.**

114 **a** Schematic representation of ATAC-seq data upstream of human *CTNNB1* gene and
 115 the location of the putative enhancer *neCTNNB1* (blue shading). **b** The Hi-C data of
 116 adult dorsolateral prefrontal Ncx were obtained from the 3D genome browser. The
 117 boundaries of TADs and locations of *neCTNNB1* and *CTNNB1* are indicated below. **b'**
 118 Regions magnified from (**b**). *neCTNNB1* interacts with *pCTNNB1* in adult dorsolateral
 119 prefrontal Ncx. **c** Virtual 4C of adult dorsolateral prefrontal Ncx revealing interactions
 120 between *neCTNNB1* and *pCTNNB1*. PFC, dorsal lateral prefrontal cortex; Motor,
 121 motor cortex; S1, primary somatosensory cortex; Temporal, temporal cortex; Parietal,
 122 parietal cortex, V1, primary visual cortex; MGE, LGE, CGE, medial, lateral, and caudal
 123 ganglionic eminences.

124

Table S1. Summary of data used in this study.

Source name	Organism	Age	Library strategy	Antibody	Serial number
Prefrontal cortex	Homo sapiens	14gw	ATAC-seq	/	GSE149268
Prefrontal cortex	Homo sapiens	17gw	ATAC-seq	/	GSE149268
Prefrontal cortex	Homo sapiens	18gw	ATAC-seq	/	GSE149268
Prefrontal cortex	Homo sapiens	19gw	ATAC-seq	/	GSE149268
Motor cortex	Homo sapiens	14gw	ATAC-seq	/	GSE149268
Motor cortex	Homo sapiens	17gw	ATAC-seq	/	GSE149268
Motor cortex	Homo sapiens	19gw	ATAC-seq	/	GSE149268
Somatosensory cortex	Homo sapiens	14gw	ATAC-seq	/	GSE149268
Somatosensory cortex	Homo sapiens	17gw	ATAC-seq	/	GSE149268
Somatosensory cortex	Homo sapiens	19gw	ATAC-seq	/	GSE149268
Temporal cortex	Homo sapiens	19gw	ATAC-seq	/	GSE149268
Parietal cortex	Homo sapiens	19gw	ATAC-seq	/	GSE149268
Visual cortex	Homo sapiens	14gw	ATAC-seq	/	GSE149268
Visual cortex	Homo sapiens	17gw	ATAC-seq	/	GSE149268
Visual cortex	Homo sapiens	19gw	ATAC-seq	/	GSE149268
Medial ganglionic eminence	Homo sapiens	14gw	ATAC-seq	/	GSE149268
Medial ganglionic eminence	Homo sapiens	18gw	ATAC-seq	/	GSE149268
Medial ganglionic eminence	Homo sapiens	19gw	ATAC-seq	/	GSE149268
Lateral ganglionic eminence	Homo sapiens	14gw	ATAC-seq	/	GSE149268
Lateral ganglionic eminence	Homo sapiens	18gw	ATAC-seq	/	GSE149268
Lateral ganglionic eminence	Homo sapiens	19gw	ATAC-seq	/	GSE149268
Caudal ganglionic eminence	Homo sapiens	14gw	ATAC-seq	/	GSE149268
Caudal ganglionic eminence	Homo sapiens	17gw	ATAC-seq	/	GSE149268
Caudal ganglionic eminence	Homo sapiens	18gw	ATAC-seq	/	GSE149268
Caudal ganglionic eminence	Homo sapiens	19gw	ATAC-seq	/	GSE149268
Prefrontal cortex	Homo sapiens	15gw	ChIP-seq	H3K27ac	GSE149268
Prefrontal cortex	Homo sapiens	17gw	ChIP-seq	H3K27ac	GSE149268
Prefrontal cortex	Homo sapiens	18gw	ChIP-seq	H3K27ac	GSE149268
Prefrontal cortex	Homo sapiens	15gw	ChIP-seq	H3K4me1	GSE149268
Forebrain	Mus musculus	E11.5	ChIP-seq	H3K27ac	ENCSR275KPI
Forebrain	Mus musculus	E15.5	ChIP-seq	H3K27ac	ENCSR691NQH
Forebrain	Mus musculus	P0	ChIP-seq	H3K27ac	ENCSR094TTT
Forebrain	Mus musculus	E11.5	DNase-seq	/	ENCSR014SFF
Forebrain	Mus musculus	E14.5	DNase-seq	/	ENCSR337EDG
Forebrain	Mus musculus	P0	DNase-seq	/	ENCSR791AJY
Forebrain	Mus musculus	E11.5	ChIP-seq	H3K4me1	ENCSR975QSF
Forebrain	Mus musculus	E15.5	ChIP-seq	H3K4me1	ENCSR875KRK
Forebrain	Mus musculus	P0	ChIP-seq	H3K4me1	ENCSR465PLB

Forebrain	Mus musculus	E11.5	ChIP-seq	H3K4me3	ENCSR739DVM
Forebrain	Mus musculus	E15.5	ChIP-seq	H3K4me3	ENCSR022KDE
Forebrain	Mus musculus	P0	ChIP-seq	H3K4me3	ENCSR258YWW
Forebrain	Mus musculus	E11.5	ChIP-seq	H3K36me3	ENCSR066LZB
Forebrain	Mus musculus	E15.5	ChIP-seq	H3K36me3	ENCSR437SFX
Forebrain	Mus musculus	P0	ChIP-seq	H3K36me3	ENCSR069TDC
Midbrain	Mus musculus	E11.5	ChIP-seq	H3K27ac	ENCSR088UKA
Midbrain	Mus musculus	E15.5	ChIP-seq	H3K27ac	ENCSR428GHF
Midbrain	Mus musculus	P0	ChIP-seq	H3K27ac	ENCSR672ZXY
Midbrain	Mus musculus	E11.5	DNase-seq	/	ENCSR292QBA
Midbrain	Mus musculus	E14.5	DNase-seq	/	ENCSR367FCW
Midbrain	Mus musculus	P0	DNase-seq	/	ENCSR767AJS
Midbrain	Mus musculus	E11.5	ChIP-seq	H3K4me1	ENCSR450ITF
Midbrain	Mus musculus	E15.5	ChIP-seq	H3K4me1	ENCSR449EUZ
Midbrain	Mus musculus	P0	ChIP-seq	H3K4me1	ENCSR391WSS
Midbrain	Mus musculus	E11.5	ChIP-seq	H3K4me3	ENCSR283RFW
Midbrain	Mus musculus	E15.5	ChIP-seq	H3K4me3	ENCSR486MHP
Midbrain	Mus musculus	P0	ChIP-seq	H3K4me3	ENCSR427ZJU
Midbrain	Mus musculus	E11.5	ChIP-seq	H3K36me3	NCSR535NVF
Midbrain	Mus musculus	E15.5	ChIP-seq	H3K36me3	ENCSR487RAU
Midbrain	Mus musculus	P0	ChIP-seq	H3K36me3	ENCSR951UWY
Hindbrain	Mus musculus	E11.5	ChIP-seq	H3K27ac	ENCSR129LAP
Hindbrain	Mus musculus	E15.5	ChIP-seq	H3K27ac	ENCSR066XFL
Hindbrain	Mus musculus	P0	ChIP-seq	H3K27ac	ENCSR332JYZ
Hindbrain	Mus musculus	E11.5	DNase-seq	/	ENCSR358ESL
Hindbrain	Mus musculus	E14.5	DNase-seq	/	ENCSR179PIH
Hindbrain	Mus musculus	P0	DNase-seq	/	ENCSR469VGZ
Hindbrain	Mus musculus	E11.5	ChIP-seq	H3K4me1	ENCSR695FPP
Hindbrain	Mus musculus	E15.5	ChIP-seq	H3K4me1	ENCSR921ILW
Hindbrain	Mus musculus	P0	ChIP-seq	H3K4me1	ENCSR617VBE
Hindbrain	Mus musculus	E11.5	ChIP-seq	H3K4me3	ENCSR928CYU
Hindbrain	Mus musculus	E15.5	ChIP-seq	H3K4me3	ENCSR335TVR
Hindbrain	Mus musculus	P0	ChIP-seq	H3K4me3	ENCSR472YGQ
Hindbrain	Mus musculus	E11.5	ChIP-seq	H3K36me3	ENCSR175QZX
Hindbrain	Mus musculus	E15.5	ChIP-seq	H3K36me3	ENCSR809NWL
Hindbrain	Mus musculus	P0	ChIP-seq	H3K36me3	ENCSR458PAO
Forebrain	Mus musculus	E12.5	ChIP-seq	P300	GSE88789
Facial prominence	Mus musculus	E15.5	ChIP-seq	H3K27ac	ENCSR382DRK
Heart	Mus musculus	E15.5	ChIP-seq	H3K27ac	ENCSR574VME
Intestine	Mus musculus	E15.5	ChIP-seq	H3K27ac	ENCSR599GVS

Kidney	Mus musculus	E15.5	ChIP-seq	H3K27ac	ENCSR711SVB
Limb	Mus musculus	E15.5	ChIP-seq	H3K27ac	ENCSR988BRP
Liver	Mus musculus	E15.5	ChIP-seq	H3K27ac	ENCSR479LFP
Lung	Mus musculus	E15.5	ChIP-seq	H3K27ac	ENCSR895BMP
Neural tube	Mus musculus	E15.5	ChIP-seq	H3K27ac	ENCSR241BSK
Stomach	Mus musculus	E15.5	ChIP-seq	H3K27ac	ENCSR929SEW
Cortical plate	Mus musculus	8 weeks	ChIP-seq	H3K27ac	ENCSR000CDD
Cortex	Mus musculus	E14.5	ChIP-seq	TBR2	GSE63621
Cortex	Mus musculus	E14.5	ChIP-seq	NEUROD2	GSE67539
Cortex	Mus musculus	E14.5	ChIP-seq	NEUROG2	GSE63621
Embryonic neural stem cells	Mus musculus	E14.5	ChIP-seq	FOXP1	GSE101632
Cortex	Mus musculus	E15	ChIP-seq	SATB2	GSE68910
Cortex	Mus musculus	E12.5	ChIP-seq	SMAD3	GSE36673
ES-derived NPCs	Mus musculus	/	ChIP-seq	SOX2	GSE35496
ES-derived NPCs	Mus musculus	/	ChIP-seq	YY1	GSE25197
AtT-20 cells	Mus musculus	/	ChIP-seq	ASH2	GSE87180
Embryonic Stem Cells	Mus musculus	E14	ChIP-seq	GFP	GSE52071
B cells	Mus musculus	6-14 weeks	ChIP-seq	ASH2	GSE20852
<i>in vitro</i> differentiated NPC	Mus musculus	/	Hi-C	/	GSE96107
Neuron	Mus musculus	E14.5	Hi-C	/	GSE96107
H1 Neuronal Progenitor cells	Homo sapiens	/	Hi-C	/	GSE52457
H1 embryonic stem cells	Homo sapiens	/	Hi-C	/	GSE52457
H1 Mesendoderm cells	Homo sapiens	/	Hi-C	/	GSE52457
H1 Trophectoderm cells	Homo sapiens	/	Hi-C	/	GSE52457
H1 Mesenchymal stem cells	Homo sapiens	/	Hi-C	/	GSE52457
Dorsolateral Prefrontal Cortex	Homo sapiens	Adult	Hi-C	/	GSE87112

<i>Ctnnb1</i> _Ex3_R	cttgccactcaggaagga	used for CHIP-qPCR
<i>neCtnnb1</i> _ctrl_F	ctgcttaagctctgccagg	used for CHIP-qPCR
<i>neCtnnb1</i> _ctrl_R	ttgacatcatggcagcttc	used for CHIP-qPCR
hDesert_F	gggagatggagaaaggtggaaggtt	used for CHIP-qPCR
hDesert_R	cccaaggccataaaaatagagctggg	used for CHIP-qPCR
<i>pCTNNB1</i> -CHIP-F	gagaggtgggatccaccatcc	used for CHIP-qPCR
<i>pCTNNB1</i> -CHIP-R	tcgccgacctgtgtgtctgtg	used for CHIP-qPCR
<i>neCtnnb1</i> -CHIP-F	gcgggcttctatccccatctg	used for CHIP-qPCR
<i>neCtnnb1</i> -CHIP-R	tgatgtggcacctcgggacc	used for CHIP-qPCR
<i>Ash2l</i> _sh1	ccttaggctatgataagttta	used for knockdown <i>Ash2l</i>
<i>Ash2l</i> _sh2	cctgtgtctgtgtgttccaaa	used for knockdown <i>Ash2l</i>
<i>ASH2L</i> _sh1	gtgactgttatcctactata	used for knockdown <i>ASH2L</i>
<i>ASH2L</i> _sh2	cctgctgtatgaacgggttt	used for knockdown <i>ASH2L</i>
<i>Ash2l</i> _F	cctactttcctcgggaagcaag	used for RT-qPCR
<i>Ash2l</i> _R	gacaatgttattggccaagtc	used for RT-qPCR
<i>ASH2L</i> _F	agaatggccgacagttggg	used for RT-qPCR
<i>ASH2L</i> _R	cctcaagtttgctgtctcc	used for RT-qPCR
<i>Ctnnb1</i> _F	atggagccggacagaaaagc	used for RT-qPCR
<i>Ctnnb1</i> _R	cttgccactcaggaagga	used for RT-qPCR
<i>CTNNB1</i> _F	aaagcggctgttagctactgg	used for RT-qPCR
<i>CTNNB1</i> _R	cgagtcattgcatactgtccat	used for RT-qPCR
<i>Satb2</i> _F	gccgtgggaggtttgatgatt	used for RT-qPCR
<i>Satb2</i> _R	accaagacgaactcagcgtg	used for RT-qPCR
<i>Neurod2</i> _F	aagccagtgtctctcgtgg	used for RT-qPCR
<i>Neurod2</i> _R	gccttggtcatcttgcgttt	used for RT-qPCR
<i>Sox2</i> _F	gcgagtggaactttgtcc	used for RT-qPCR
<i>Sox2</i> _R	cgggaagcgtgtacttatcctt	used for RT-qPCR
<i>Yy1</i> _F	cagtggttgaagagcagatcat	used for RT-qPCR
<i>Yy1</i> _R	agggagttcttgcctgtcat	used for RT-qPCR
<i>Gapdh</i> _F	aggtcgggtgaacggatttg	used for RT-qPCR
<i>Gapdh</i> _R	tgtagaccatgtagttgaggta	used for RT-qPCR
<i>Ctnnb1</i> ^{lox(ex3)} -F	ggtagtggccctgcccttgacac	used for validation of <i>Ctnnb1</i> ^{lox(ex3)} mice
<i>Ctnnb1</i> ^{lox(ex3)} -AS5	acgtctggcaagttccgcgtcatcc	used for validation of <i>Ctnnb1</i> ^{lox(ex3)} mice
<i>Ctnnb1</i> ^{lox(ex3)} -P85	ctaagcttggtggacgtaaacctc	used for validation of <i>Ctnnb1</i> ^{lox(ex3)} mice
<i>Ctnnb1</i> ^{KO} -WT-F	ccctgcccctgcatatagcatttga	used for validation of <i>Ctnnb1</i> ^{KO} mice
<i>Ctnnb1</i> ^{KO} -WT-R	ccccacctgtgatgctttgatgtct	used for validation of <i>Ctnnb1</i> ^{KO} mice
<i>Ctnnb1</i> ^{KO} -Mut-R	atgctgtgtgagtgaccctactcct	used for validation of <i>Ctnnb1</i> ^{KO} mice
LacZ F	atcctctgcatggtcaggtc	used for validation of <i>neCtnnb1</i> -LacZ-iCre and BAT-Gal mice
LacZ R	cgtggcctgattcattcc	used for validation of <i>neCtnnb1</i> -LacZ-iCre and BAT-Gal mice